The Astrophysical Journal Letters, 979:L9 (10pp), 2025 January 20 https://doi.org/10.3847/2041-8213/ada0bd

The Hubble Tension in Our Own Backyard: DESI and the Nearness of the Coma Cluster

Daniel Scolnic[1], Adam G. Riess[2,3], Yukei S. Murakami[3], Erik R. Peterson[1], Dillon Brout[4], Maria Acevedo[1], Bastien Carreres[1], David O. Jones[5], Khaled Said[6,7], Cullan Howlett[6,7], and Gagandeep S. Anand[8]
[1] Department of Physics, Duke University, Durham, NC 27708, USA
[2] Space Telescope Science Institute, Baltimore, MD 21218, USA
[3] Department of Physics and Astronomy, Johns Hopkins University, Baltimore, MD 21218, USA
[4] Departments of Astronomy and Physics, Boston University, Boston, MA 02140, USA
[5] Institute for Astronomy, University of Hawai'i, 640 North A'ohoku Place, Hilo, HI 96720, USA
[6] School of Mathematics and Physics, University of Queensland, Brisbane, QLD 4072, Australia
[7] OzGrav: The ARC Centre of Excellence for Gravitational Wave Discovery, Hawthorn, VIC 3122, Australia
[8] Space Telescope Science Institute, 3700 San Martin Drive, Baltimore, MD 21218, USA
Received 2024 September 23; revised 2024 November 24; accepted 2024 December 03; published 2025 January 15

Abstract

The Dark Energy Spectroscopic Instrument (DESI) collaboration measured a tight relation between the Hubble constant (H_0) and the distance to the Coma cluster using the fundamental plane (FP) relation of the deepest, most homogeneous sample of early-type galaxies. To determine H_0, we measure the distance to Coma by several independent routes, each with its own geometric reference. We measure the most precise distance to Coma from 13 Type Ia supernovae (SNe Ia) in the cluster with a mean standardized brightness of $m_B^0 = 15.710 \pm 0.040$ mag. Calibrating the absolute magnitude of SNe Ia with the Hubble Space Telescope (HST) distance ladder yields $D_{\rm Coma} = 98.5 \pm 2.2$ Mpc, consistent with its canonical value of 95–100 Mpc. This distance results in $H_0 = 76.5 \pm 2.2\,{\rm km\,s^{-1}\,Mpc^{-1}}$ from the DESI FP relation. Inverting the DESI relation by calibrating it instead to the Planck+ΛCDM value of $H_0 = 67.4\,{\rm km\,s^{-1}\,Mpc^{-1}}$ implies a much greater distance to Coma, $D_{\rm Coma} = 111.8 \pm 1.8$ Mpc, 4.6σ beyond a joint, direct measure. Independent of SNe Ia, the HST Key Project FP relation as calibrated by Cepheids, the tip of the red giant branch from JWST, or HST near-infrared surface brightness fluctuations all yield $D_{\rm Coma} < 100$ Mpc, in joint tension themselves with the Planck-calibrated route at $>3\sigma$. From a broad array of distance estimates compiled back to 1990, it is hard to see how Coma could be located as far as the Planck+ΛCDM expectation of >110 Mpc. By extending the Hubble diagram to Coma, a well-studied location in our own backyard whose distance was in good accord well before the Hubble tension, DESI indicates a more pervasive conflict between our knowledge of local distances and cosmological expectations. We expect future programs to refine the distance to Coma and nearer clusters to help illuminate this new local window on the Hubble tension.

Unified Astronomy Thesaurus concepts: Type Ia supernovae (1728); Distance measure (395); Distance indicators (394)

1. Introduction

The "Hubble tension" refers to the discrepancy in the value of the Hubble constant, H_0, between multiple measures of local distance and redshift (clustering around $H_0 \sim 73\,{\rm km\,s^{-1}\,Mpc^{-1}}$) versus an inferred value based on measurements of the cosmic microwave background (CMB) and the standard model of cosmology (found to be around $H_0 \sim 67.5\,{\rm km\,s^{-1}\,Mpc^{-1}}$); see L. Verde et al. (2024) for a review. As there is not yet an accepted theory of new physics to explain this discrepancy, there has been a wide focus on new and improved ways to study this phenomenon.

Recently, the Dark Energy Spectroscopic Instrument (DESI) collaboration (K. Said et al. 2024, hereafter S24) measured a tight relation between the Hubble constant (H_0) and the distance to the Coma cluster using the fundamental plane (FP) relation of the deepest, most homogeneous sample of early-type galaxies (DESI Collaboration et al. 2024). The FP is a long-known relation for early-type galaxies between their velocity dispersion, surface brightness, and apparent radius (S. Djorgovski & M. Davis 1987; A. Dressler et al. 1987) that adds a parameter and tightens the earlier Faber–Jackson relation between their velocity and luminosity (S. M. Faber & R. E. Jackson 1976). The DESI measurement consists of redshifts and uncalibrated FP distances to 4191 early-type galaxies in the Hubble flow and 226 such FP distances in the Coma cluster. DESI measures the Hubble flow at $0.023 < z < 0.1$, and Coma serves only as a reference location, rich in early-type galaxies, where the uncalibrated FP distances may be calibrated from knowledge of the distance to Coma. S24 found $H_0 = 76.05 \pm 0.35$ (statistical) $\pm$ 0.49 (systematic FP) $\pm$ 4.86 (FP calibration) $\rm km\,s^{-1}\,Mpc^{-1}$, a result usefully described as

$$H_0 = (76.05 \pm 1.3) * \left(\frac{99.1\ \ {\rm Mpc}}{D_{\rm Coma}}\right)\ \ {\rm km\,s^{-1}\,Mpc^{-1}}. \quad (1)$$

The DESI FP relation estimate of H_0 depends on knowledge of the distance to Coma that was obtained by S24 from a surface brightness fluctuation (SBF) measurement of one galaxy in Coma, $D_{\rm Coma} = 99.1 \pm 5.8$ Mpc (J. B. Jensen et al. 2021; hereafter J21). The uncertainty from the DESI measurement is modest at $\pm 1.3\,{\rm km\,s^{-1}\,Mpc^{-1}}$ (dominated by the FP relation measurement of 226 galaxies in Coma) so that the uncertainty in the DESI estimate of H_0 is dominated by

knowledge of the distance to Coma, one of the richest nearby clusters in the local Universe ($z = 0.023$; M. D'Onofrio et al. 1997). Our Letter attempts to improve on this uncertainty by measuring the distance to Coma with a new sample of a dozen Type Ia supernovae (SNe Ia) in the cluster and by leveraging other distance measurements from the Hubble Space Telescope (HST) and the James Webb Space Telescope (JWST) to improve the H_0 constraint.

Coma has a long history of distance measurements to the objects within it. A historical compilation of distance measurements was presented in R. de Grijs & G. Bono (2020),[9] and a compilation from the 1990s–2000s is given in D. Carter et al. (2008), including the use of Tully–Fisher, SBF, $D_n - \sigma$, FP, and globular clusters, resulting in an average of $D_{\rm Coma} \sim 95$ Mpc. The HST Key Project (KP) calibrated the FP relation in nearby clusters (Virgo, Fornax, and Leo I) and Coma, which resulted in a measured distance of 86 ± 8 Mpc (D. D. Kelson et al. 2000; W. L. Freedman et al. 2001; R. de Grijs & G. Bono 2020). Coma is generally too far to reach directly with primary distance indicators (i.e., Cepheids, tip of the red giant branch (TRGB) stars, Miras, J-region asymptotic giant branch (JAGB) stars, blue supergiant stars), but it is rich in early-type galaxies, which are ideal targets for SBF or galaxy-based methods like the FP relation.

SNe Ia offer an especially capable tool for calibrating the distance to the Coma cluster. With canonical rates of one SN per galaxy per 100 yr, we should expect on the order of ~tens of SNe in Coma to have been discovered by various surveys over the last decade. The most recent effort to collect SNe Ia in Coma came from a 1990 study, "Distances of the Virgo and Coma Clusters of Galaxies through Novae and Supernovae" (M. Capaccioli et al. 1990), which gathered five from the 1960s and 1970s going back to F. Zwicky (1961); however, the quality of these data by modern standards is quite poor. A precise distance measurement requires multiple SNe Ia whose light curves and spectra pass contemporary quality cuts from photometric systems that are well characterized with additional samples in the Hubble flow for empirical testing. Until the last decade, Coma was not continuously searched for transients, so many past SNe Ia would have been missed. The Pantheon+ compilation (D. Brout et al. 2022; D. Scolnic et al. 2022) contains only two SNe Ia located in Coma. Recent surveys like the Asteroid Terrestrial-impact Last Alert System (ATLAS; J. L. Tonry et al. 2018; K. W. Smith et al. 2020) and the Zwicky Transient Facility (ZTF; E. C. Bellm et al. 2019) cover large fractions of the northern sky. This includes the area of the Coma cluster at R.A. = 13 hr and decl. = 28°, and queries of their databases indicate they have found >10 SNe Ia around Coma in the last few years.

In Section 2, we search for SNe located within the Coma cluster with publicly available catalogs and light curves. We then fit the light curves in Section 3 to derive standardized brightnesses of the SNe. In Section 4, we measure a precise distance to Coma based on the calibrations of the absolute luminosity of SNe Ia. Combining with other methods independent of SNe Ia, we also measure H_0 using the DESI measurements of S24. Our discussion and conclusions are given in Sections 5 and 6.

2. Data

Given our goal of measuring a reliable distance to Coma, we collect SNe Ia whose membership in Coma can be established with high confidence by their three-dimensional coordinates and with data suitable for high-quality distance measurements. In order to ascertain whether SNe Ia may be located in the Coma cluster, we first determine the size and location of the cluster from a sample of virially associated galaxies. Following E. R. Peterson et al. (2022), we query the "group" catalog that defines groups of galaxies in the nearby Universe ($z < 0.04$) from R. B. Tully (2015, hereafter T15), as well as the new full Coma group catalog from S24 and the subset of these galaxies used in S24 to determine FP measurements. We show the galaxy members according to these three subsamples in Figure 1 (left). The catalogs share a common boundary and a common redshift range of $0.015 < z < 0.032$, both with a median heliocentric redshift of ~0.0232 and standard deviation of 0.003. The center (R.A., decl.) for both catalogs is (~195°, ~28°).

From T15, the Coma group contains 148 members, and from the full DESI Coma group, the group contains 1696 members. T15 is limited to brighter, larger members, but they are sufficient as a cross-check for defining the inner bound region of Coma with high confidence. The incompleteness from T15, as discussed in E. R. Peterson et al. (2024), is due to the magnitude-limited galaxy surveys used to make up the group catalogs. These catalogs provide the redshift range of the group as listed above, as well as the spatial contours in R.A. and decl., which are presented in Figure 1. We find that an ellipse with a center (195°, 28°) with a semimajor R.A. axis of 3.°5, a semiminor decl. axis of 2°, and an angle of 15° encloses all of the galaxy members of these catalogs. The right panel of Figure 1 highlights the region with the highest concentration of galaxies within the cluster.[10]

Given the constraints in redshift and location from the group catalog, we query the Transient Name Server[11] (TNS) and SIMBAD (M. Wenger et al. 2000) for spectroscopically confirmed SNe Ia. We query for SNe post-1990 from multiple servers, though note that TNS appears to be incomplete for years before 2015, and SIMBAD is incomplete for years after 2020. We find 32 spectroscopically confirmed SNe Ia within the ellipse as shown in Figure 1 and report their names, positions, host-galaxy positions, and heliocentric redshifts in the Appendix. The majority of SNe discovered after 2018 were found/measured by ATLAS and ZTF, as well as a smaller number by the Young Supernova Experiment (YSE; D. O. Jones et al. 2021; public data release, P. D. Aleo et al. 2023). We retain all spectroscopically normal SNe Ia with high-quality light curves following well-established quality criteria (D. Scolnic et al. 2015); see the Appendix for further details. All SNe included in our main analysis are associated with a host galaxy in the S24 full group catalog, with the exception of 2020ags and 2022frn, which appear to be "hostless." Still, the redshifts of these two SNe are within the nominal redshift range for Coma and within the ellipse outlined above.

[9] Two mean distances are provided by R. de Grijs & G. Bono (2020) for Coma, 99.5 Mpc by absolute measures or 90.4 Mpc for measures relative to Virgo. Importantly, we note that they cite only the dispersion of all measures rather than the error in their mean, which would require an analysis of their correlated terms that the authors do not undertake. The error in the mean is also needed for comparisons, so we only cite their mean here.

[10] https://www.astrobin.com/full/fh0dto/C/

[11] https://www.wis-tns.org/

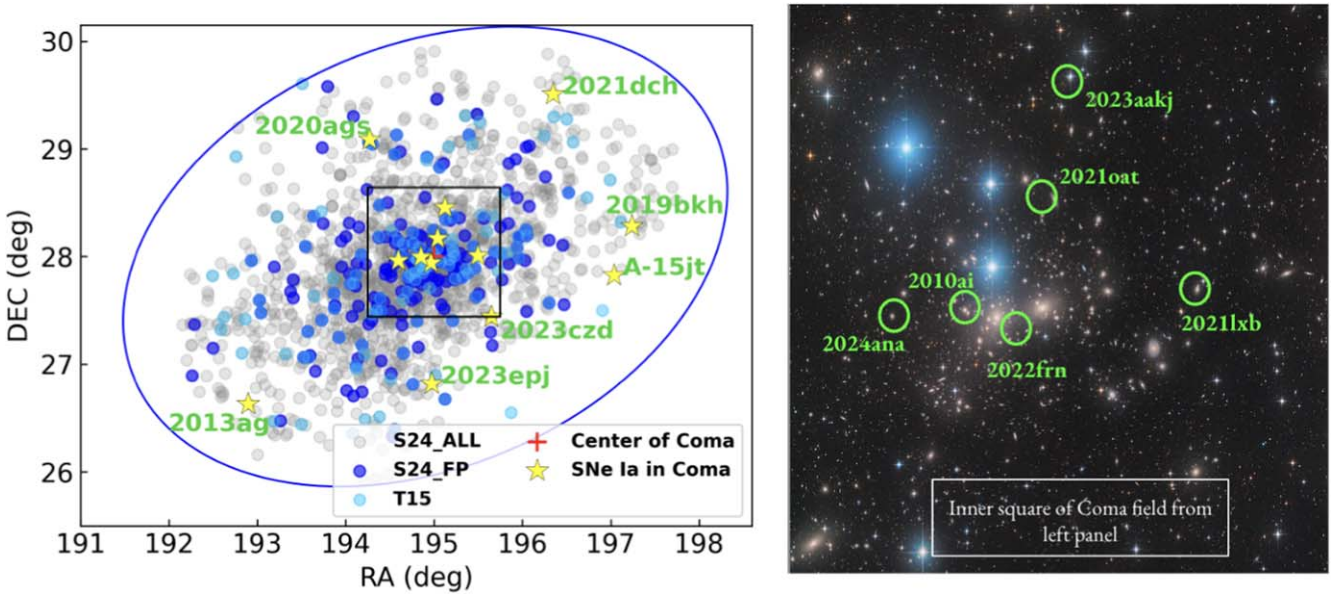

Figure 1. (Left) The locations of the SNe Ia identified to be in the Coma cluster (yellow stars) and the galaxies identified to be in the Coma group as from the full S24 Coma group catalog (light gray circles), the S24 FP sample (dark blue circles), and the T15 Coma group catalog (light blue circles). The center of the cluster is marked in red. The positions of the SNe are listed in Table 1. (Right) For the rectangular box on the left, a colored image of that sky area with the SNe within that location marked.

We provide an example light curve from the ATLAS database for an SN Ia in Coma in Figure 2; we also show the stamp of the host galaxy of the SN. We share all the light-curve data and figures like Figure 1 for each SN on GitHub,[12] with a copy deposited to Zenodo: 10.5281/zenodo.14213131. We find three SNe already in the Pantheon+ compilation that are located in the cluster: 2010ai, 2013ag, and ASASSN-15jt. Both ATLAS and YSE photometry are photometrically calibrated to the Pan-STARRS (K. C. Chambers et al. 2016) AB magnitude system. YSE photometry was measured with the Pan-STARRS telescope (K. C. Chambers et al. 2016), and thus previous system characterization (e.g., R. J. Foley et al. 2018; D. Scolnic et al. 2022) can be used. Since the ATLAS and YSE photometric systems are relatively new and less studied, we undertake an additional procedure, remeasuring the Hubble flow with each, to check for survey offsets in the following section.

3. Measuring a Mean Standardized Brightness for SNe Ia in the Coma Cluster

3.1. Light-curve Fitting and Standardization

We use the SALT2 light-curve model (introduced in J. Guy et al. 2010; modified in D. Brout et al. 2022) to be consistent with past H_0 measurements as described in the Pantheon +SH0ES analysis (D. Brout et al. 2022). We apply light-curve quality requirements as described in D. Scolnic et al. (2022), which can be summarized as a SALT2 color c within $(-0.3, 0.3)$, a SALT2 stretch x_1 within $(-3, 3)$, measurements in two filters with a signal-to-noise ratio >5, and at least one measurement before peak and spectroscopically classified as a normal SN Ia (following Pantheon+, including SN Ia-91T, excluding SN Ia-91bg). Of the 32 SNe from the literature search, there are 12 SNe with light curves that are publicly available and pass the SALT2 fit and the quality checks. One, 2021lxb, was observed by both ATLAS and YSE. The most common reason for failure was due to inadequate coverage from multiple bands. An explanation of why specific SNe Ia did not pass the cuts is included in the Appendix.

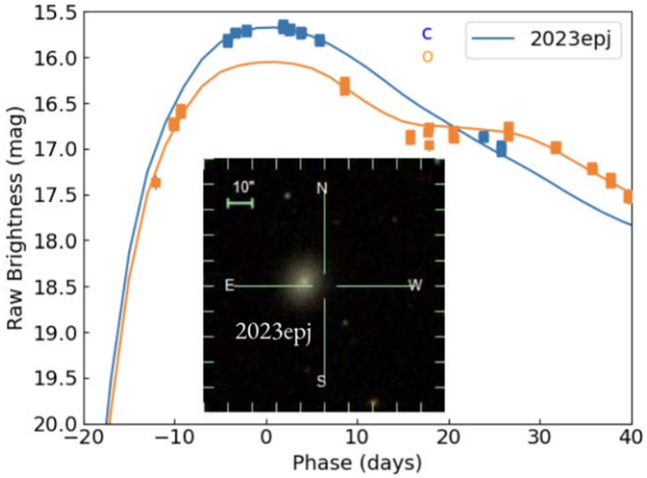

Figure 2. Raw light-curve data in the "c" and "o" bands from the ATLAS survey of one representative SN: 2023epj. The curves are the SALT2 model fit. The inset shows the position of the SN relative to its host galaxy (K. N. Abazajian et al. 2009). This figure for each SN Ia, along with the raw data, is online at GitHub, https://github.com/dscolnic/Coma, and Zenodo, 10.5281/zenodo.14213131.

We show the positions of all the SNe Ia that pass the cuts in Figure 1. We present the SALT2 fit parameters (m_B, x_1, c) in Table 1. In Pantheon+, the standardized brightness m_B^0 was calculated by

$$m_B^0 = m_B + 0.15x_1 - 3.1c - \delta_B, \quad (2)$$

where the multiplicative coefficients for stretch and color were determined in Pantheon+ to minimize the Hubble residual dispersion.

[12] https://github.com/dscolnic/Coma

Table 1
Properties of SNe Ia in Coma and Their Light Curves

SN	z_{hel}[a]	P-SN[b]	P-Host[b]	m_B	x_1	c	Host Log Mass	δ_B	m_B^0
ATLAS SNe									
2019bkh	0.0195	197.2391 28.2812	197.2381 28.2804	15.96 ± 0.03	0.76 ± 0.07	0.09 ± 0.02	9.40	0.04	15.76 ± 0.17
2020ags	0.0206	194.2706 29.0887	– – – [c]	15.46 ± 0.02	0.09 ± 0.07	−0.06 ± 0.01	7.80	0.05	15.60 ± 0.12
2021dch	0.0202	196.34900 29.5096	196.3484 29.5104	15.99 ± 0.03	−1.42 ± 0.06	−0.08 ± 0.03	9.55	0.08	15.94 ± 0.13
2021lxb[d]	0.0259	195.4944 28.0086	195.4900 28.0058	16.75 ± 0.05	−2.13 ± 0.08	0.22 ± 0.03	11.07	−0.12	15.86 ± 0.28
2022frn	0.0230	194.9657 27.9435	– – – [c]	15.93 ± 0.02	−1.28 ± 0.07	−0.02 ± 0.02	7.51	0.04	15.76 ± 0.13
2023aakj	0.0241	195.1214 28.4555	195.1223 28.4557	15.66 ± 0.07	−1.52 ± 0.06	−0.21 ± 0.04	9.13	0.22	15.86 ± 0.15
2023czd	0.0180	195.6467 27.4393	195.6465 27.4394	15.31 ± 0.03	0.36 ± 0.06	−0.08 ± 0.02	9.50	0.07	15.54 ± 0.11
2023epj	0.0267	194.9738 26.8194	194.9764 26.8200	15.36 ± 0.01	0.33 ± 0.06	−0.12 ± 0.01	9.62	0.12	15.67 ± 0.12
2024ana	0.0201	194.5941 27.9662	194.5908 27.9678	16.31 ± 0.03	−2.44 ± 0.08	0.07 ± 0.02	9.97	−0.00	15.75 ± 0.17
YSE SNe									
2021lxb[d]	0.0259	195.4944 28.0086	195.4900 28.0058	16.58 ± 0.04	−2.29 ± 0.04	0.14 ± 0.03	11.07	−0.05	15.84 ± 0.22
2021oat	0.0225	195.0344 28.1703	195.0378 28.1704	15.22 ± 0.04	−0.04 ± 0.07	−0.18 ± 0.03	10.19	0.14	15.65 ± 0.14
Pantheon+ SNe									
2010ai	0.0183	194.8501 27.9964	194.8544 27.9967	15.68 ± 0.04	−1.65 ± 0.09	−0.12 ± 0.03	9.11	0.08	15.73 ± 0.10
2013ag	0.0213	192.8959 26.6293	192.8987 26.6295	15.80 ± 0.04	−1.11 ± 0.75	0.02 ± 0.06	8.79	0.01	15.57 ± 0.21
ASASSN-15jt	0.02306	197.0380 27.8264	197.0381 27.8265	16.75 ± 0.04	−2.33 ± 0.143	0.21 ± 0.04	9.91	0.07	15.64 ± 0.22

Notes.
[a] The heliocentric redshifts are all from the host-galaxy spectra ($\sigma_z = 0.0001$) except in the cases of 2020ags and 2022frn, which do not have obvious hosts. The redshift for these SNe Ia comes from the SN spectra themselves and $\sigma_z = 0.005$.
[b] Positions of the SN and host galaxy, respectively.
[c] No host associated within 15".
[d] 2021lxb is the only SN with light curves from two samples.

The term, δ_B, known as a "bias correction," is a standard measure of the difference between the the population mean and the statistical selection of an SN Ia sample as predicted from simulations of discovery and follow-up (R. Kessler & D. Scolnic 2017). More recently, this includes a function that accounts for (i.e., simulates) the empirical correlation between standardized SN Ia brightness and host-galaxy mass (D. Brout & D. Scolnic 2021). Hosts masses are given in Table 1 and are derived for this sample following the approximation determined in E. N. Taylor et al. (2011) and photometry from K. C. Chambers et al. (2016). To measure bias corrections following R. Kessler & D. Scolnic (2017), we simulate the ATLAS and YSE samples with the SNANA package (R. Kessler et al. 2009). We generate properties of the survey directly from the light-curve data of the respective samples and determine a selection function so that the redshift distribution between the simulation and data match. We follow the simulation methodology in D. Brout et al. (2022) and use the intrinsic scatter model developed in B. Popovic et al. (2021) that describes the observed color as a mix of intrinsic color, dust reddening, and noise. The uncertainty on the magnitudes is determined following R. Kessler & D. Scolnic (2017) and is dependent on the fitted SALT2 c and x_1 of each SN. The mean of the bias corrections is larger than average samples, 0.048 ± 0.021 mag, due to 6 of the 13 light curves having $c \leqslant -0.08$ (D. Brout et al. 2022). These less dusty, blue SNe are more common in ellipticals common to clusters (R. Chen et al. 2022), and standardization is biased for the bluest SNe due to the use of a single color–luminosity standardization coefficient (i.e., 3.1 in Equation (2)) as discussed in D. Scolnic & R. Kessler (2016). If we split the sample in half, sorted by the bias-correction size, the offset in m_B^0 between the two subsamples is 0.0 ± 0.08 mag.

When we compare 38 SNe common to the full samples of both YSE and ATLAS SNe (i.e., not limited to Coma), we find a difference in SN color of 0.04 mag. This is not surprising, as the ATLAS "*co*" bands are novel and different than the common *griz* (YSE) or *BVRI* filters used and well studied for most SN Ia samples. We attribute this difference to a modest misestimate of the preliminary calibration of the ATLAS "*c*" band, a finding further indicated by comparing the ATLAS color distributions between simulations and data, and add the 0.04 mag to the ATLAS "*c*"-band photometry.

We present all the standardized brightness values of the SNe in Coma in Table 1 and Figure 3. We find very good agreement for the standardized brightnesses measured for the SNe in and around the cluster. The range of magnitudes for the 13 SNe is

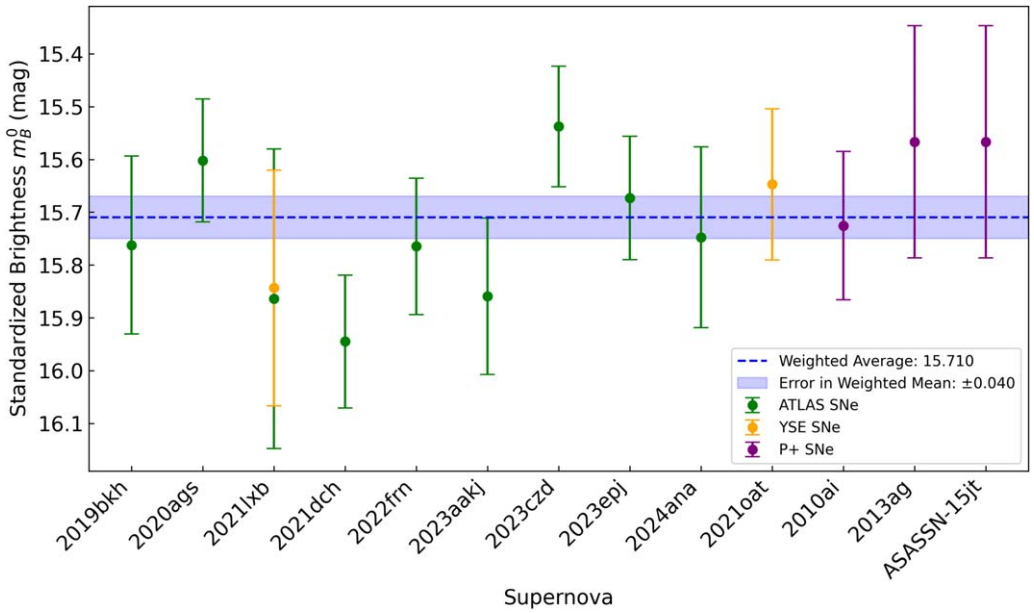

Figure 3. Standardized magnitudes for SNe Ia in the Coma cluster whose light curves pass quality cuts. The average line is shown in dashed blue. The colors of the SNe are tied to the survey sample.

15.54–15.94 mag. The SN, 2021lxb, which is common to both the YSE and ATLAS samples, has a difference in standardized brightness between the two of 0.02 mag; we therefore use the light curve from YSE, as the standardized brightness has a smaller uncertainty. Weighting for the individual uncertainties, we measure an average standardized brightness derived from Equation (2) for 12 SNe Ia in Coma to be

$$\bar{m}_B^0 = 15.710 \pm 0.040 \text{ mag}. \quad (3)$$

3.2. Checking Accuracy of Measurements

First, we check that the calibration of the YSE and ATLAS samples are consistent with samples used in Pantheon+ (so that we can tie to the absolute calibration determined there). We follow the methodology in S. Brownsberger et al. (2023) to check whether mean standardized SNe Ia magnitudes in different samples produce the same magnitude at a given redshift. This is accomplished by comparing the calculated Hubble diagram intercept (a_B) for ATLAS and YSE in bins to that found for the full sample used in A. G. Riess et al. (2022, hereafter R22) of $a_B = 0.714 \pm 0.002$. The a_B calculation is

$$a_B = \log\Big(cz\Big[1 + \tfrac{1}{2}(1 - q_0)z - \tfrac{1}{6}(1 - q_0 - 3q_0^2 + j_0)z^2\Big]\Big) + O(z^3) - 0.2m_B^0. \quad (4)$$

We note that a_B need not be used to solve for survey offsets but is an effective summarization of the mean magnitude of a sample. We find very good agreement (at an a_B level of 0.002) inferred for YSE and ATLAS compared to that from Pantheon +, implying remaining calibration differences on the ~0.01 mag level, which is negligible compared to the statistical uncertainty when added in quadrature.

The total χ^2 measured for Figure 3 is $\chi^2 = 8.9$ for the average of 13 individual SNe with a sample dispersion of 0.12 mag, similar to that found for SN Ia samples in the Hubble flow (e.g., the Pantheon+ dispersion is 0.13 mag). Monte Carlo simulations of the same number of SNe show that a χ^2 this low or lower should happen ~20% of the time for 13 SNe.

As discussed in the Appendix, two SNe, 1994S and 2020jhf, are both within the angular range but right at the low-redshift limit and are not included, as they may be in front of the cluster. These two SNe are 1.0 and 0.5 mag brighter, respectively, than the mean. Inclusion of these two SNe would reduce the Coma distance by ~0.10 mag (and as discussed in the next section, increase H_0). Another SN excluded from the sample, 2015M, is classified (M. Hicken et al. 2007) as super-Chandrasekhar (D. A. Howell et al. 2006) and appears to be a 3σ outlier compared to the other brightnesses in Table 1. There are two SNe, 2019be and 2006bz, that would produce fainter mean values if included but are cut by the x_1 requirement and are also classified as 1991bg-like (B. Leibundgut et al. 1993), a peculiar SN Ia subtype routinely excluded in cosmological samples (D. Scolnic et al. 2022). Because there is greater volume beyond Coma than in front of it, statistical inclusion of nonmembers would tend to overestimate the standardized brightness. Future, larger samples of SNe in Coma may benefit from a simultaneous analysis of membership and standardized brightness. For this sample, we note both the conservative membership and our uncertainty in the mean (in the sense that we used the larger, expected errors rather than renormalizing them by the lower dispersion of the sample).

We check to see if there is any relation between any of the properties of the SNe Ia and the standardized brightness. We calculate trends between m_B^0 and the following properties: redshift, separation between SN and host positions, separation from the center of the cluster, host mass, and the x_1 and c fit parameters. We do not find significant evidence for a nonzero slope; the lowest p-value, expressing the chance that a recovered slope is consistent with zero, is only as low as 19%.

The one possible trend with standardized brightness is from a correlation with x_1. We note that our sample does have a high relative fraction of fast-declining SNe (low x_1 values); this is likely due to the fact that more SNe are found in ellipticals in a

cluster, and those SNe are more often fast-declining (M. Sullivan et al. 2010; R. Chen et al. 2022). We measure a small dependence of the standardized brightness on x_1 in our sample of $-0.066 \pm 0.038\,\mathrm{mag}/x_1$, which is $<2\sigma$. This trend may be indicative of the "broken–α" relation found in P. Garnavich et al. (2023) and later M. Ginolin et al. (2024), though these did not account for the impact of bias corrections. To understand this further, first, we verify that fast-declining SNe Ia are standardized without significant bias by checking those in the Pantheon+ sample and find that the mean Hubble residual for $x_1 < -1.3$ is $+0.01 \pm 0.02$ mag, not indicative of a bias. Second, instead of fitting a slope to our Coma sample, we measure the difference in standardized brightness when we split the sample at a range of values from $x1 = -1.5$ to $x1 = -0.5$. We see differences in standardized brightness as large as 0.16 ± 0.08 (2σ) mag and as small as 0.08 ± 0.08 (1σ) mag. As there is no obvious residual bias from the Pantheon+ sample, and any discrepancies in our Coma sample are at most 2σ, we do not include an additional systematic uncertainty, though this will be important to monitor with a larger Coma sample in the future.

As a cross-check of the mean standardized brightness found here, we examine the Pantheon+ Hubble diagram to measure the mean standardized brightness for SNe at the redshift of the Coma cluster. We measure the CMB-frame redshift of the Coma cluster from the group catalog as shown in Figure 1 and find the mean to be 0.02422, and the median is 0.02445 ± 0.00024. If we query the Pantheon+ sample for SNe with CMB redshifts within 0.005 of 0.02422, we find a mean magnitude of $m_{B,\mathrm{corr}} = 15.71 \pm 0.022$, in $<1\sigma$ agreement with that directly found for SNe in the Coma cluster. This indicates that the mean redshift of the Coma cluster is accurately measured using the group average and that calibration/bias-correction differences between the new samples and the Pantheon+ sample are likely limited to the ~0.03 mag level. We thus consider our mean result in Equation (3) as robust and representative of the mean standardized brightness of a SN Ia in the Coma cluster.

4. The Distance to Coma

4.1. Converting SN Ia Brightness into Distance

The luminosities of standardized SNe Ia, M_B, have been calibrated by other standard candles (e.g., Cepheids or TRGB, themselves calibrated geometrically) so that we can measure the distance (modulus) to Coma,

$$\mu = m_B^0 - M_B. \tag{5}$$

The most precise measurement of M_B for SNe Ia (and with Pantheon+ standardization) comes from the calibration of 42 SNe Ia with measurements of HST Cepheids and four geometric anchors (R22). As shown in A. G. Riess et al. (2024) and with measurements from W. L. Freedman et al. (2024) for the largest JWST samples, HST Cepheids yield consistent distances (to within ~1σ) with eight other methods or telescope samples: JWST Cepheids, TRGB, and JAGB by two groups, plus HST TRGB and Miras. We take the baseline value from R22 of $M = -19.253 \pm 0.027$ mag; then, following Equation (5), we measure a distance modulus to Coma of 34.97 ± 0.05 mag. This can be directly converted into a distance to Coma following

$$\mathrm{Distance\ (Mpc)} = 10^{0.2\times(\mu-25)}, \tag{6}$$

resulting in $D_{\mathrm{Coma}} = 98.5 \pm 2.2$ Mpc. We note that this is significantly closer, by 4.2σ, than the expected result of $\mu = 35.24 \pm 0.039$ or $D_{\mathrm{Coma}} = 111.8 \pm 1.8$ Mpc if the DESI Hubble relation is instead calibrated with $H_0 = 67.4 \pm 0.5\,\mathrm{km\,s^{-1}\,Mpc^{-1}}$ from Planck+ΛCDM (. This distance results in $H_0 = 76.5 \pm 2.2\,\mathrm{km\,s^{-1}\,Mpc^{-1}}$ from the DESI FP relation. The difference between this and the result from the HST distance ladder, $H_0 = 73.0 \pm 1.0\,\mathrm{km\,s^{-1}\,Mpc^{-1}}$, removing error terms in common, is $3.5 \pm 2.3\,\mathrm{km\,s^{-1}\,Mpc^{-1}}$, 1.5σ.

4.2. Non-SN Distance to Coma

There have been numerous studies of the distance to Coma and we summarize them in Table 2. An extensive review of more than 60 distance measurements to Coma going back more than five decades is presented in R. de Grijs & G. Bono (2020); see Figure 4. We exclude those based on the use of redshift and assumption for a value of the Hubble constant to avoid circularity. These distance estimates demonstrate a tightening of the range in the last 20 yr. We narrow the focus to a smaller compilation of more recent literature by D. Carter et al. (2008, their Table 1), which gives distances from six studies: *I*-band Tully–Fisher (R. B. Tully & M. J. Pierce 2000), *K*-band SBF (J. B. Jensen et al. 1999), *I*-band SBF (B. Thomsen et al. 1997), $D_n - \sigma$ (M. D. Gregg 1997), FP (J. Hjorth & N. R. Tanvir 1997), and globular cluster luminosity function (GCLF; J. J. Kavelaars et al. 2000). These have a mean of $D_{\mathrm{Coma}} = 95.1 \pm 3.1$ Mpc and are consistent as a set with a $\chi^2 = 5.9$ for the six values, indicating reasonable consensus. We do not attempt to determine the correlated terms in the D. Carter et al. (2008) sample but rather defer that step to a combination of more recent measures in the next section.

The HST KP undertook a study of the FP for early-type galaxies in a range of nearby galaxy clusters and in Coma (D. D. Kelson et al. 2000). In principle, this is a logical extension of the DESI FP measure of the Hubble flow calibrated to Coma but to even nearer galaxy clusters via the same tool. By measuring the FP relations in three local clusters, Virgo, Fornax, and Leo I, with 26 galaxies, D. D. Kelson et al. (2000) established a zero-point for the FP, calibrated by the HST KP Cepheid data set and 81 galaxies in Coma from I. Jorgensen et al. (1995a, 1995b). The random and systematic uncertainties in the FP are given by D. D. Kelson et al. (2000) as 0.02 dex (5% in distance) and 0.03 dex (7% in distance), respectively. The updated Cepheid zero-point error including the LMC detached eclipsing binary (DEB) distance is 4% (G. Pietrzyński et al. 2019). The result is an updated HST KP FP Coma distance estimate of $\mu = 34.67 \pm 0.21$ mag or 85 ± 8 Mpc, including systematic uncertainties as summarized by R. de Grijs & G. Bono (2020).

The TRGB-SBF Project has recently measured with JWST the distance to the same three local clusters used by the HST KP to measure the Coma distance. Using the values given in G. S. Anand et al. (2024a, 2024b) to recalibrate the HST KP FP relation results in 90 ± 9 Mpc. Lastly, we include in Table 2 the HST near-infrared (NIR) SBF estimate of the Coma distance from J21 used by S24 (DESI), 99.1 ± 5.8 Mpc, based on a single galaxy.

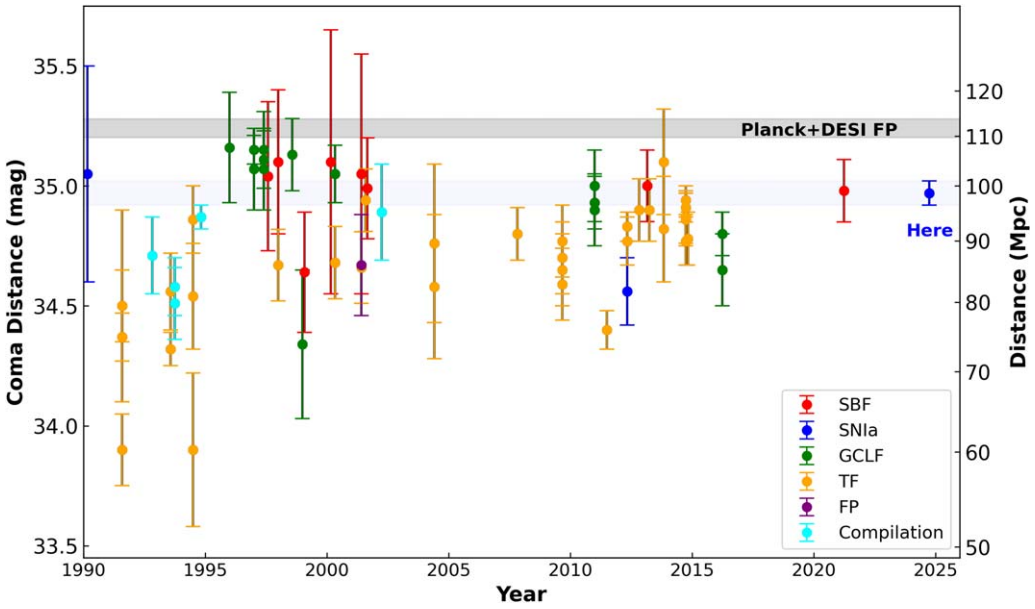

Figure 4. Historical (1990 onward) distance modulus measurements of the Coma cluster (as reviewed in R. de Grijs & G. Bono 2020). Only distance measurements that do not depend on redshift and H_0 are included.

Table 2
The Distance to Coma Determined by Various Methods

Technique	Distance (Mpc)	Distance Modulus (mag)	Reference
Literature Compilation (D. Carter et al. 2008)			
I-band Tully–Fisher	86.3 ± 6	34.68 ± 0.15	R. B. Tully & M. J. Pierce (2000)
K'-band SBF	85 ± 10	34.64 ± 0.27	J. B. Jensen et al. (1999)
I-band SBF	102 ± 14	35.04 ± 0.32	B. Thomsen et al. (1997)
$D_n - \sigma$	96 ± 6	34.90 ± 0.14	M. D. Gregg (1997)
FP	108 ± 12	35.16 ± 0.25	J. Hjorth & N. R. Tanvir (1997)
GCLF	102 ± 6	35.05 ± 0.12	J. J. Kavelaars et al. (2000)
Literature mean	95 ± 3.1	34.89 ± 0.06	
HST KP FP[a]	85 ± 8	34.67 ± 0.21	D. D. Kelson et al. (2000); W. L. Freedman et al. (2001)
JWST TRGB+FP	90 ± 9	34.74 ± 0.18	G. S. Anand et al. (2024a)
HST NIR SBF	99.1 ± 5.8	34.98 ± 0.13	J21
SH0ES Cepheids+SNe Ia	98.5 ± 2.2	34.97 ± 0.05	Here
Combination of independent	98.0 ± 2.0	34.965 ± 0.045	Here

Note.
[a] See R. de Grijs & G. Bono (2020), who update the HST KP Cepheid calibration of LMC 18.50 ± 0.13 with the DEB result of 18.477 ± 0.026 mag from G. Pietrzyński et al. (2019).

4.3. Combining Independent Techniques

We can increase the precision of the measurement from an average of *uncorrelated* measurements from the most recent distance measurements to Coma. For each measurement, we describe the calibration ladder to reach Coma. The J21 distance to Coma in Table 2 is based on SBF, which is calibrated by Cepheids measured by the HST KP, and these Cepheids are calibrated by the DEB distance to the LMC (G. Pietrzyński et al. 2019). The JWST TRGB measurements from G. S. Anand et al. (2024a, 2024b) may be used to recalibrate the HST KP FP from the same three local clusters, Virgo, Fornax, and Leo I, and then follow the same FP link to Coma. The JWST TRGB itself is calibrated by NGC 4258 (M. J. Reid et al. 2019). Lastly, for the combination analyzed in this Letter, we may adopt the calibration of SNe Ia by SH0ES Cepheids, which are calibrated only by Gaia EDR3 Milky Way parallaxes (R22; fit 11 in their Table 5).

The distance constraint from combining these three independent measurements is $D_{\rm Coma} = 98.0 \pm 2.0$ Mpc or $\mu_0 = 34.957 \pm 0.045$ mag. Using Equation (1) converts this into $H_0 = 76.9 \pm 2.0\,{\rm km\,s^{-1}\,Mpc^{-1}}$. We show these independent approaches as well as the combination in Figure 5. As also shown in Figure 5, the distance found from combining these local measurements is ~4.6σ (0.28 ± 0.06 mag) from the distance to Coma of $D = 111.8 \pm 1.8$ Mpc if one combines the DESI FP Hubble relation with the H_0 from Planck+ΛCDM of $67.4\,{\rm km\,s^{-1}\,Mpc^{-1}}$.

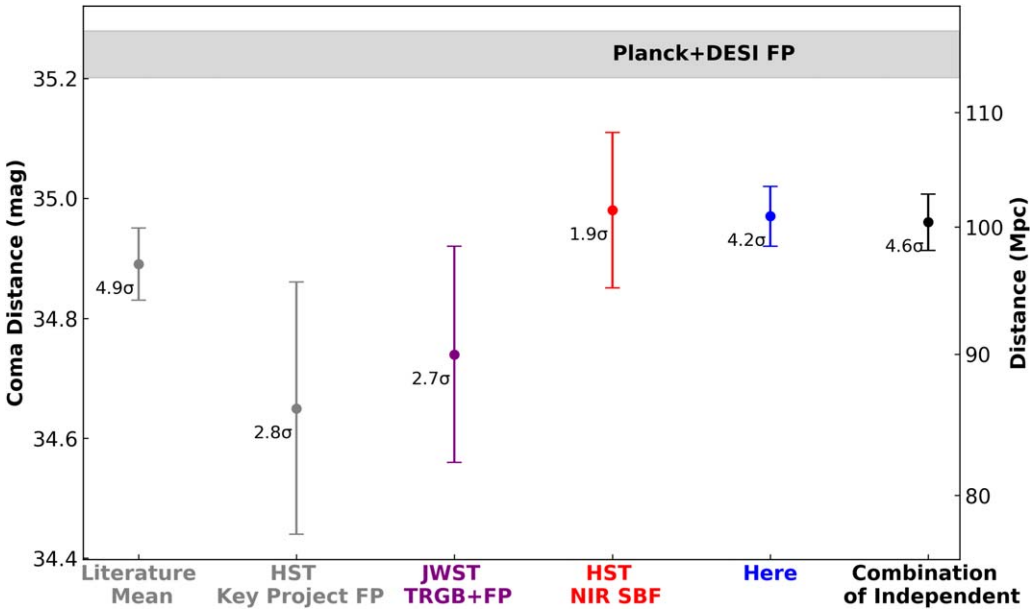

Figure 5. The distance modulus measurements to the Coma cluster as summarized in Table 2. "Combination of Independent" refers to combining JWST TRGB+FP, HST NIR SBF, and the Cepheid+SN Ia measurement from this Letter, all independent techniques (three colored points).

5. Discussion

Although the Hubble tension is seen as a difference in the most precise local and inferred measurements of the Hubble constant, it appears likely that the issue is more pervasive. There appears to be a broad conflict with long-accepted distances to the nearest objects versus that inferred via the inverse, cosmological distance ladder. Unlike most local distance ladders, which rely on custom-measured distances to relatively obscure galaxies, with the DESI FP, the conflict is now seen as "baked-in," existing a priori of the Hubble tension in the long history of distance measurements to Coma and without reference to any one source, method, group, or metric. Rather than simply a conflict between two sets of measurements, it appears likely to extend to our preexisting knowledge of local distances measured independently of their redshifts. As the inverse distance ladder is extended ever closer to home, we may see a broadening of the set of distance indicators that can be used to test it. We expect future DESI releases to amplify the issue by improving statistics while connecting the Hubble flow to even closer clusters, such as Fornax, Virgo, Leo I, etc.

5.1. Additional Potential Sources of Uncertainty

One source of uncertainty not discussed in this analysis is the radial size of the Coma cluster itself. E. L. Łokas & G. A. Mamon (2003) calculate that the radial size is 2.86 Mpc, which is ~3% of the distance to Coma. Following B. Carreres et al. (2024) and E. R. Peterson et al. (2024), we check the size of large clusters like Coma in Uchuu *N*-body simulations and find that large clusters like Coma have a typical radial size of ~2 Mpc, in rough agreement. J21 measure the distance to a single galaxy, NGC 4874, which is one of the two brightest and most massive galaxies in the cluster, likely near the center of the galaxy cluster. Assuming that the galaxies DESI measures the FP relation with are evenly distributed across the cluster, the difference between the mean location of the 226 FP relation galaxies measured and the center is likely a small fraction of the 2.86 Mpc radial size.

For the present analysis, we measure distances to 13 SNe spread across the cluster. As shown in Figure 1, 6 of the 13 are likely located in the central core of the cluster. The difference in mean brightness between the inner core and outer core is 0.077 ± 0.080 mag, a $<1\sigma$ difference (SNe near the core being fainter). Assuming that the distribution of SNe discovered is relatively uniform across the cluster or that it roughly traces the distribution of galaxies used for FP relation measurements, we should likewise expect this fractional difference in position along the Coma cluster to be subdominant to the other uncertainties in the Coma distance measurement.

We include both the statistical and systematic uncertainties in the FP relation from S24, and from Figure 8 of S24, we note that variants in their analysis that relate to the FP relation measurement could change the inferred distance of Coma by at most 3%. S24 also extensively studied different bulk-flow models and noted that their impact is on the ~1% level for H_0 or distance. To reconcile the canonical distance to Coma and the DESI FP relation with the Planck value of H_0, the mean peculiar velocity would need to be $\sim -950\,\mathrm{km\,s^{-1}}$, much larger than the mean of $\sim -20\,\mathrm{km\,s^{-1}}$ derived from bulk-flow models for the cluster (A. Carr et al. 2022).

5.2. Future Prospects

S24 anticipate that the forthcoming set of DESI year 1 FP relation data (Ross et al., in preparation) will be substantially larger (4000 versus ~100,000 elliptical galaxies), which will reduce both the statistical and systematic uncertainties. In addition, the upcoming DESI data should extend the FP relation to multiple nearer clusters besides Coma, such as Fornax, Virgo, and Leo I, and given the success of the current analysis for one cluster, it is likely that various distance measurements (e.g., SNe, Cepheids, TRGB) can all be used to directly reach these clusters.

As shown in the Appendix, from 2019 to 2024, 18 SNe Ia were discovered and spectroscopically confirmed to be SNe Ia in Coma, a rate of several per year. A number of the light curves for these SNe are sparse, and a commitment to

Table 3
Coma and H_0 Uncertainties in a DESI-based Distance Ladder

Source	Value (mag)	Reference
SN Ia M_B	0.027	R22
Coma SN Ia m_B	0.040	Here
Coma distance subtotal	0.049	
FP in Coma ($N = 226$)[a]	0.033	S24
FP in Hubble flow ($N = 4191$) +DESI sys.	0.017	S24
Local subtotal (H_0)	0.063	
Planck+ΛCDM	0.013	Planck Collaboration et al. (2020)
Comparison total	0.064[b]	

Notes.
[a] Each FP relation distance has an uncertainty of 23% (S24).
[b] Using the independent combination of distance measurements for Coma results in a reduced total of 0.061 mag. This comparison total uncertainty applies when comparing a Coma distance calibrated locally with DESI versus a Coma distance calibrated with Planck+DESI.

multiband, high-cadence photometric follow-up for SNe in clusters like Coma would be strongly beneficial. Additionally, in the last 5 yr, according to TNS, 81 likely SNe were discovered in the area of Coma (not accounting for a redshift cut that can be found in the ellipse of Figure 1). Only 29 of the 81 received a spectroscopic identification. A commitment to spectroscopic follow-up for identification could roughly double the number of usable SNe Ia compared to the last 5 yr. As shown in Table 3, the uncertainty in the mean of SNe Ia in Coma is the largest uncertainty in the error budget. With ~40 SNe Ia measured, or fewer with better measurements, the uncertainty in the mean would be ~0.024 mag, smaller than the uncertainty in the current calibration between SNe Ia and Cepheids and smaller than the FP relation measurement of 226 galaxies in Coma.

6. Conclusions

In this analysis, we calibrated 13 high-quality light curves of SNe Ia located in the Coma cluster, yielding a standardized SN Ia brightness of $\overline{m_B^0} = 15.710 \pm 0.040$ mag and the highest-precision distance to the Coma cluster to date. The HST distance ladder calibration (R22) of the SN Ia luminosity places Coma at 34.97 ± 0.05 mag, or a distance of 98.5 ± 2.2 Mpc, consistent with historical measurements but with ~2–3× the precision of any recent individual measure. The inverse distance ladder of the Hubble diagram from the DESI FP relation combined with H_0 as measured with Planck+ΛCDM places Coma at a significantly larger distance of $D = 111.8 \pm 1.8$ Mpc, 4.2σ beyond this direct measure and well beyond the consensus distance. Alternatively, combining uncorrelated local distance measurements to Coma with the DESI measurement, we find $H_0 = 76.9 \pm 2.0\,\mathrm{km\,s^{-1}\,Mpc^{-1}}$, 4.6σ from the Planck value. This new route, the Coma distance and DESI Hubble diagram, yields another vantage point for the Hubble tension, seen here from an even broader range of local distance indicators and independent of the SN Ia measuring the Hubble flow. Based on this study of Coma or of compilations over the last several decades, it is hard to see how Coma could be located as far as the cosmological expectation of 110–115 Mpc.

There are good prospects for improving upon this result in the near term. Upcoming JWST programs have targeted Coma for intensive measurements (PI: Jensen; GO 5989) in Cycle 3 (2025). In addition, dedicated spectroscopic and photometric follow-up of SNe in the Coma cluster can easily improve on the present result. It is likely that within just a few years, the uncertainty in H_0 from a Coma-based distance ladder will be dominated not by uncertainties from measurements within Coma but rather the calibration of those measurements elsewhere in this new distance ladder.

Acknowledgments

We thank the Templeton Foundation for directly supporting this research. D.S. is supported by Department of Energy grant DE-SC0010007, the David and Lucile Packard Foundation, the Templeton Foundation, and the Sloan Foundation. D.O.J. acknowledges support from NSF grant AST-2407632 and NASA grant 80NSSC24M0023.

This research used data obtained with the Dark Energy Spectroscopic Instrument (DESI). DESI construction and operations are managed by the Lawrence Berkeley National Laboratory. This material is based upon work supported by the U.S. Department of Energy, Office of Science, Office of High-Energy Physics, under contract No. DE–AC02–05CH11231, and by the National Energy Research Scientific Computing Center, a DOE Office of Science User Facility, under the same contract. Additional support for DESI was provided by the U.S. National Science Foundation (NSF), Division of Astronomical Sciences, under contract No. AST-0950945 to the NSF's National Optical-Infrared Astronomy Research Laboratory; the Science and Technology Facilities Council of the United Kingdom; the Gordon and Betty Moore Foundation; the Heising-Simons Foundation; the French Alternative Energies and Atomic Energy Commission (CEA); the National Council of Science and Technology of Mexico (CONACYT); the Ministry of Science and Innovation of Spain (MICINN), and the DESI Member Institutions: www.desi.lbl.gov/collaborating-institutions. The DESI collaboration is honored to be permitted to conduct scientific research on Iolkam Du'ag (Kitt Peak), a mountain with particular significance to the Tohono O'odham Nation. Any opinions, findings, and conclusions or recommendations expressed in this material are those of the author(s) and do not necessarily reflect the views of the U.S. National Science Foundation, the U.S. Department of Energy, or any of the listed funding agencies.

Appendix

We include here a comprehensive list in Table 4 of all SNe found in our TNS and SIMBAD queries and whether they are included in the sample, and if not, the reason. “Unavailable” means there is no light-curve photometry available. “Too sparse” means there is a light curve but only a small number of epochs. The rest of the notes should be self-explanatory.

Two SNe Ia in Pantheon+, 1994S and 2020jhf, have redshifts right near the lower redshift limit of 0.015 ($z = 0.01524$ and 0.015371, respectively), and we do not include them, as they may be in front of the cluster; the next lowest redshift of an SN Ia is $z = 0.018$. One SN, 2015M, near the center of the cluster and well within the redshift range at $z = 0.02316$, is classified as super-Chandrasekhar-like (M. Hicken et al. 2007) from its spectrum (i.e., peculiar); this

Table 4
SNe Ia Discovered in Coma, Sorted by Redshift

Name	R.A. (deg)	Decl. (deg)	z_{hel}	Note
1994S	187.8410	29.1344	0.0152	Very bright, in front of cluster
2020jhf	198.7227	27.0086	0.0154	Very bright, in front of cluster
2023czd	195.6467	27.4393	0.0180	In sample
2010ai	194.8501	27.9964	0.0184	In sample
2019bkh	197.2389	28.2813	0.0195	In sample
2021wad	195.1308	28.3464	0.0199	Not enough data
2019be	195.0604	27.9568	0.02	No light curve, 91bg-like
2020ags	194.2706	29.0887	0.02	In sample
2024ana	194.5941	27.9662	0.0201	In sample
2013ag	192.8959	26.6293	0.0213	In sample
2021dch	196.3490	29.5096	0.0202	In sample
ASASSN-16bg	194.8546	27.7403	0.0202	Unavailable
ASASSN-16np	189.1800	26.1135	0.0208	Unavailable
2024rkc	198.3561	27.794	0.0210	Unavailable
ASASSN-14bd	193.1867	26.4703	0.0213	Unavailable
2016iuc	198.3608	27.8068	0.0214	Unavailable
2024fxl	190.1514	26.5059	0.0220	Only one filter
ASASSN-15jt	197.0380	27.8263	0.0222	In sample
2021oat	195.0344	28.1703	0.0225	In sample
2022frn	194.9657	27.9435	0.023	In sample
2015M	195.1346	27.9781	0.0232	Outlier, super-Chandrasekhar
2020afp	193.9218	27.2500	0.0237	x_1 cut, 91bg-like
2001cg	193.9203	27.2511	0.0240	Too sparse
2023aakj	195.1214	28.4555	0.0241	In sample
2021lxb	195.4944	28.0086	0.0259	In sample
2023ke	194.5760	29.1287	0.0260	Missed peak
PTF 11gdh	195.1586	28.0567	0.0262	Unavailable
2023epj	194.9738	26.8194	0.0267	In sample
2006bz	195.1808	27.9616	0.0277	x_1 cut, 91bg-like
2009L	194.7004	27.6738	0.0280	Unavailable
2006cg	196.2597	28.7400	0.0288	Too sparse
2003an	201.9731	28.5081	0.0327	Unavailable

SN is much brighter than others in Coma and is thus not included in our list.

ORCID iDs

Daniel Scolnic https://orcid.org/0000-0002-4934-5849
Adam G. Riess https://orcid.org/0000-0002-6124-1196
Erik R. Peterson https://orcid.org/0000-0001-8596-4746
Dillon Brout https://orcid.org/0000-0001-5201-8374
Maria Acevedo https://orcid.org/0000-0002-5389-7961
David O. Jones https://orcid.org/0000-0002-6230-0151
Khaled Said https://orcid.org/0000-0002-1809-6325
Cullan Howlett https://orcid.org/0000-0002-1081-9410
Gagandeep S. Anand https://orcid.org/0000-0002-5259-2314

References

Abazajian, K. N., Adelman-McCarthy, J. K., Agüeros, M. A., et al. 2009, ApJS, 182, 543
Aleo, P. D., Malanchev, K., Sharief, S., et al. 2023, ApJS, 266, 9
Anand, G. S., Tully, R. B., Cohen, Y., et al. 2024a, ApJ, 973, 83
Anand, G. S., Tully, R. B., Cohen, Y., et al. 2024b, arXiv:2408.16810
Bellm, E. C., Kulkarni, S. R., Graham, M. J., et al. 2019, PASP, 131, 018002
Brout, D., & Scolnic, D. 2021, ApJ, 909, 26
Brout, D., Scolnic, D., Popovic, B., et al. 2022, ApJ, 938, 110
Brownsberger, S., Brout, D., Scolnic, D., Stubbs, C. W., & Riess, A. G. 2023, ApJ, 944, 188
Capaccioli, M., Cappellaro, E., della Valle, M., et al. 1990, ApJ, 350, 110
Carr, A., Davis, T. M., Scolnic, D., et al. 2022, PASA, 39, e046
Carreres, B., Rosselli, D., Bautista, J. E., et al. 2024, arXiv: 2405.20409
Carter, D., Goudfrooij, P., Mobasher, B., et al. 2008, ApJS, 176, 424
Chambers, K. C., Magnier, E. A., Metcalfe, N., et al. 2016, arXiv: 1612.05560
Chen, R., Scolnic, D., Rozo, E., et al. 2022, ApJ, 938, 62
de Grijs, R., & Bono, G. 2020, ApJS, 248, 6
DESI Collaboration, Adame, A. G., Aguilar, J., et al. 2024, AJ, 168, 58
Djorgovski, S., & Davis, M. 1987, ApJ, 313, 59
D'Onofrio, M., Capaccioli, M., Zaggia, S. R., & Caon, N. 1997, MNRAS, 289, 847
Dressler, A., Faber, S. M., Burstein, D., et al. 1987, ApJL, 313, L37
Faber, S. M., & Jackson, R. E. 1976, ApJ, 204, 668
Foley, R. J., Scolnic, D., Rest, A., et al. 2018, MNRAS, 475, 193
Freedman, W. L., Madore, B. F., Gibson, B. K., et al. 2001, ApJ, 553, 47
Freedman, W. L., Madore, B. F., Jang, I. S., et al. 2024, arXiv:2408.06153
Garnavich, P., Wood, C. M., Milne, P., et al. 2023, ApJ, 953, 35
Ginolin, M., Rigault, M., Smith, M., et al. 2024, arXiv:2405.20965
Gregg, M. D. 1997, NewA, 1, 363
Guy, J., Sullivan, M., Conley, A., et al. 2010, A&A, 523, A7
Hicken, M., Garnavich, P. M., Prieto, J. L., et al. 2007, ApJL, 669, L17
Hjorth, J., & Tanvir, N. R. 1997, ApJ, 482, 68
Howell, D. A., Sullivan, M., Nugent, P. E., et al. 2006, Natur, 443, 308
Jensen, J. B., Blakeslee, J. P., Ma, C.-P., et al. 2021, ApJS, 255, 21
Jensen, J. B., Tonry, J. L., & Luppino, G. A. 1999, ApJ, 510, 71
Jones, D. O., Foley, R. J., Narayan, G., et al. 2021, ApJ, 908, 143
Jorgensen, I., Franx, M., & Kjaergaard, P. 1995a, MNRAS, 273, 1097
Jorgensen, I., Franx, M., & Kjaergaard, P. 1995b, MNRAS, 276, 1341
Kavelaars, J. J., Harris, W. E., Hanes, D. A., Hesser, J. E., & Pritchet, C. J. 2000, ApJ, 533, 125
Kelson, D. D., Illingworth, G. D., van Dokkum, P. G., & Franx, M. 2000, ApJ, 531, 159
Kessler, R., Becker, A. C., Cinabro, D., et al. 2009, ApJS, 185, 32
Kessler, R., & Scolnic, D. 2017, ApJ, 836, 56
Leibundgut, B., Kirshner, R. P., Phillips, M. M., et al. 1993, AJ, 105, 301
Łokas, E. L., & Mamon, G. A. 2003, MNRAS, 343, 401
Peterson, E. R., Carreres, B., Carr, A., et al. 2024, arXiv:2408.14560
Peterson, E. R., Kenworthy, W. D., Scolnic, D., et al. 2022, ApJ, 938, 112
Pietrzyński, G., Graczyk, D., Gallenne, A., et al. 2019, Natur, 567, 200
Planck Collaboration, Aghanim, N., Akrami, Y., et al. 2020, A&A, 641, A1
Popovic, B., Brout, D., Kessler, R., Scolnic, D., & Lu, L. 2021, ApJ, 913, 49
Reid, M. J., Pesce, D. W., & Riess, A. G. 2019, ApJL, 886, L27
Riess, A. G., Yuan, W., Macri, L. M., et al. 2022, ApJL, 934, L7
Riess, A. G., Scolnic, D., Anand, G. S., et al. 2024, ApJ, 977, 120
Said, K., Howlett, C., Davis, T., et al. 2024, arXiv:2408.13842
Scolnic, D., Brout, D., Carr, A., et al. 2022, ApJ, 938, 113
Scolnic, D., Casertano, S., Riess, A., et al. 2015, ApJ, 815, 117
Scolnic, D., & Kessler, R. 2016, ApJL, 822, L35
Smith, K. W., Smartt, S. J., Young, D. R., et al. 2020, PASP, 132, 085002
Sullivan, M., Conley, A., Howell, D. A., et al. 2010, MNRAS, 406, 782
Taylor, E. N., Hopkins, A. M., Baldry, I. K., et al. 2011, MNRAS, 418, 1587
Thomsen, B., Baum, W. A., Hammergren, M., & Worthey, G. 1997, ApJL, 483, L37
Tonry, J. L., Denneau, L., Heinze, A. N., et al. 2018, PASP, 130, 064505
Tully, R. B. 2015, AJ, 149, 171
Tully, R. B., & Pierce, M. J. 2000, ApJ, 533, 744
Verde, L., Schöneberg, N., & Gil-Marìn, H. 2024, ARA&A, 62, 287
Wenger, M., Ochsenbein, F., Egret, D., et al. 2000, A&AS, 143, 9
Zwicky, F. 1961, PASP, 73, 185